Results in Physics 15 (2019) 102626

Contents lists available at ScienceDirect

Results in Physics

journal homepage: www.elsevier.com/locate/rinp

Computational studies of mono-chalcogenides ZnS and ZnSe at high-pressures

S. Ferahtia, S. Saib, N. Bouarissa*

Laboratory of Materials Physics and its Applications, University of M'sila, 28000 M'sila, Algeria

ARTICLE INFO

Keywords:
ZnS
ZnSe
Electronic structure
Elastic constants
Thermal properties
High-pressure

ABSTRACT

A pseudopotential study of structural, electronic, elastic and thermodynamic properties of mono-chalcogenides ZnS and ZnSe has been reported. Two phases such as zinc-blende and rocksalt are considered here. The computations are essentially based on the density functional theory within the local density approximation. Physical quantities such as elastic constants and phonon dispersions have been presented. The lattice constants, bulk modulus, entropy and heat capacity and their temperature dependence are analyzed and discussed. Furthermore, the effect of high pressure on the features under investigation of the materials in question is examined.

Introduction

The II–VI semiconductor compounds have received many of attention. This is due to their appealing fundamental properties. Their technological applications range from optoelectronic devices [1–12] to luminescence biological tags [13,14]. Zinc sulfide (ZnS) and zinc selenium (ZnSe) belong to this family of materials and crystallize in the zinc-blende structure at zero pressure [15–17]. They are important materials in the semiconductor devices manufacture. ZnS has been of great interest because of its polymorphic structural transformation. Besides, the material in question found optoelectronic applications in blue-light domain [18]. ZnSe in its zinc-blende structure has an energy gap of 2.70 eV [19]. It is perfectly suited for the fabrication of blue light emitting diodes as well as quantum well devices [20]. The material of interest can also find applications in a large transmission wavelength range as an infrared optical material.

The fundamental properties of ZnX compounds have been studied using methods of varying degree of sophistication [15–27]. To cite a few, Benmakhlouf and Bouarissa [18] have used a pseudopotential approach so as to study ZnS electronic properties. Agrawal et al. [24] performed first-principles calculations in order to obtain the band structure and its derived structural and vibrational properties of semiconductors based on Zn. Casali and Christensen [28] have reported the results of elastic constants of ZnS, ZnSe and ZnTe under high compression using the full-potential linear muffin–tin orbitals method.

High pressure is considered to be one of key tools which can be used to discover and access novel phases and new properties of semiconductors [29–33]. Besides, the understanding of the mechanism of transition from zinc-blende to rocksalt [34–45] becomes an important subject which has useful technological applications. It is also important for the control of the transition process. Hence, the present study can shed some light onto this interesting issue. Similarly to temperature, pressure is an important parameter which play a key role in determining the thermodynamics of semiconductors. As a matter of fact, the effect of pressure is different from that of temperature in such a way that it affects overall interatomic and intermolecular distances which in turn affects the density. The variation in inter-atomic distances permits the scan of the atomic and molecular interactions and reveals exotic fundamental properties.

This work deals with a theoretical study of fundamental properties of ZnS and ZnSe in both zinc-blende and rocksalt phases at different applied pressures. The objective of this work is to show to what extent the hydrostatic pressure can affect the structural, electronic, elastic, vibrational and thermodynamic properties of ZnS and ZnSe giving thus novel properties of these materials which may have use in various device applications. First, we calculate structural parameters. Then we have determined the electronic structure. In the next part we calculate the elastic and the thermodynamic parameters of the materials being considered here. The pressure effect on the studied properties is also investigated to further clarify the variation the ZnS and ZnSe properties under compression. Finally, a summary of the main results are given.

Computational approach

The calculations are carried out using the abinit code [46]. The latter permits the use of the pseudopotential plane-wave method within

* Corresponding author.
E-mail address: nadir.bouarissa@univ-msila.dzn (N. Bouarissa).

https://doi.org/10.1016/j.rinp.2019.102626
Received 4 July 2019; Received in revised form 27 August 2019; Accepted 27 August 2019
Available online 30 August 2019

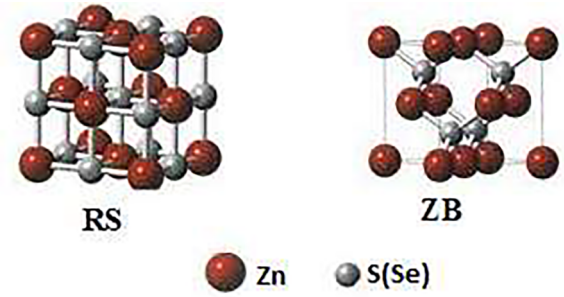

Fig. 1. Crystal structures of rocksalt (RS) and zinc-blende (ZB) ZnS(Se) semiconductor compounds.

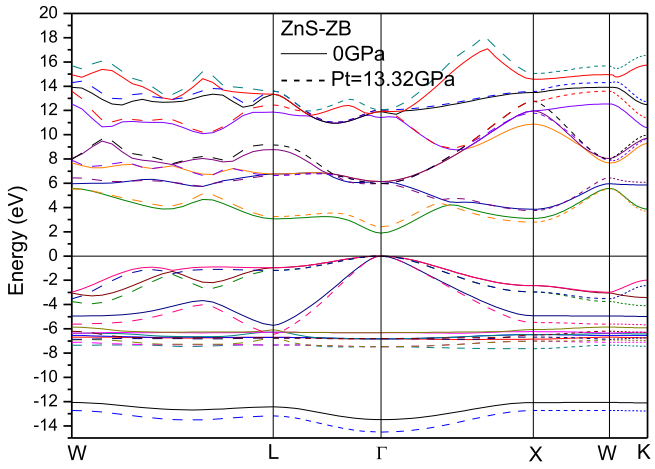

Fig. 2a. Electronic band structure for zinc-blende (ZB) ZnS at zero and under pt pressures.

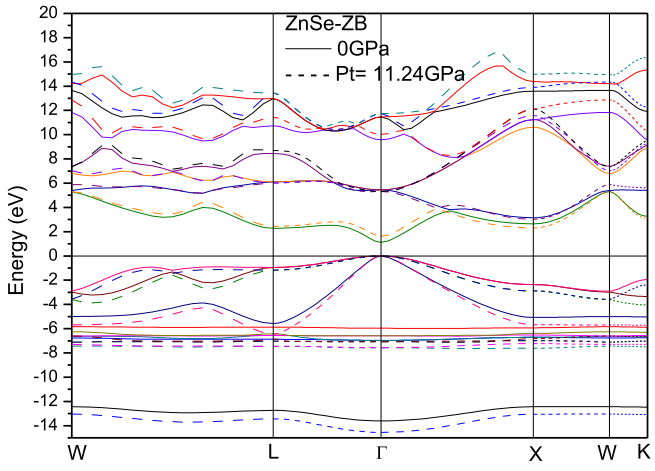

Fig. 2b. Electronic band structure for zinc-blende (ZB) ZnSe at zero and under pt pressures.

the local-density approximation (LDA) based on the density functional theory (DFT). The exchange–correlation functional of Ceperley–Alder [47] has been chosen. A Troullier- Martin type norm conserving pseudopotentials has been considered [48]. An energy cutoff of 90 Ry is used. For sampling the Brillouin zone, a 6 × 6 × 6 Monkhorst-Pack [49] special *k*-meshes have been used. This was sufficient for the total

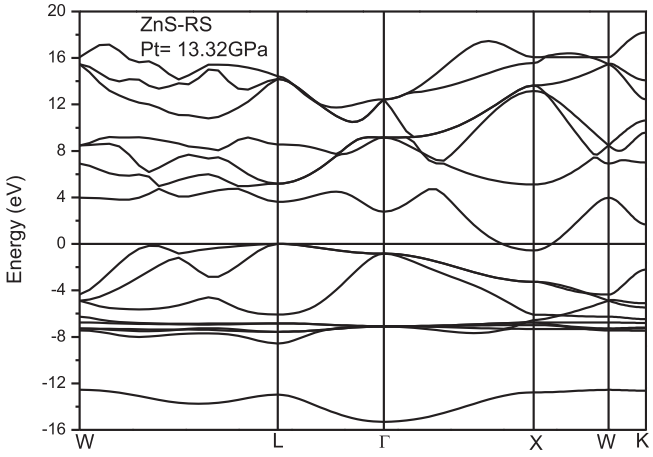

Fig. 3a. Electronic band structure for rocksalt (RS) ZnS at 13.32 GPa.

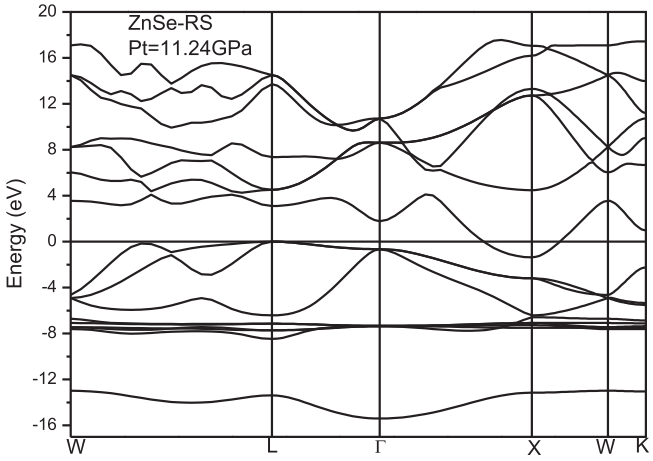

Fig. 3b. Electronic band structure for rocksalt (RS) ZnSe at 11.24 GPa.

energy convergence with an accuracy of around 1 mRy per formula unit. The elastic constants are calculated through a total energy approach based on the density functional perturbation theory (DFPT). The use of the linear response approach [50–53] has led to the calculation of the phonon frequencies and atomic displacements. This has avoided the use of supercells and allowed the computation of the dynamical matrix at arbitrary q vectors. As regards the vibrational properties, meshes of 4 × 4 × 4 have been used. The corresponding energy cutoff is140 Ry. The convergence of the phonon frequencies is ensured to be within 2 cm^{-1}.

To compute the thermodynamic properties, we have considered the dipole–dipole interaction in the inter-atomic force constants calculation. More calculation details about the phonon modes at the centre of the Brillouin zone and the thermodynamic properties were given in our recent published work [54].

The transition pressures (pt) between zinc-blende (B3 phase) to rocksalt (B1 phase) of ZnS and ZnSe are determined by considering the energies as a function of the unit cell volume, E(V), and then taking the slope of the tangent common to the two E(V) curves.

Table 1
Lattice parameter a_0, Bulk modulus B_0 and its pressure derivative B_0' of ZnS and ZnSe for zinc-blende and rocksalt phases.

Material		Zinc-blende			Rocksalt		
		a_0(Å)	B_0 (GPa)	B_0'	a_0(Å)	B_0 (GPa)	B_0'
ZnS	This work	5.33	83.16	4.337	4.988	102.93	4.362
	Expt.	5.41 [63]	76.9 [63]	3.6 [63]	5.06 [37]	103.6 [37]	4.0 [37]
	Theor,	5.311 [56]	87.835 [56]	4.84 [56]	5.07 [25]	89.54 [25]	4.58 [25]
ZnSe	This work	5.604	68.54	4.42	5.21	84.91	5.055
	Expt.	5.67 [64]	62.5 [64]	3.7 [64]	5.299 [21]	104 [21]	–
	Theor,				5.268 [22]	88.5 [22]	4.28 [22]
					5.172 [23] 90.72 [23] 4.92 [23]	90.72 [23]	4.92 [23]

Table 2
Elastic constants of ZnS and ZnSe for zinc-blende and rocksalt phases.

P(GPa)		Zinc-blende			Rocksalt			Reference
		C_{11}	C_{12}	C_{44}	C_{11}	C_{12}	C_{44}	
ZnS	0	108.83	68.18	45.50	174.17	72.06	54.23	This work
		104 [70]	65 [70]	46.2 [70]				Expt.
		122 [71]	68 [71]	57 [71]				Theor.
	Pt	147.21	115.24	41.70				This work
ZnSe	0	86.99	53.37	35.48				This work
		85.9 [70]	50.6 [70]	40.6 [70]				Expt.
		91.2 [71]	58.2 [71]	42 [71]				Theor.
	Pt	119.92	92.25	33.85				This work

Results and discussion

Electronic properties

Fig. 1 shows the crystal structures of rocksalt and zinc-blende ZnS (Se) semiconductor compounds referred to in the remaining figures as RS and ZB, respectively.

Electronic band structures at zero and at pressure of transition (pt) from zinc-blende structure to rocksalt structure (13.32 GPa for ZnS and 11.24 GPa for ZnSe) are computed and plotted in Figs. 2a, 2b and 3a, 3b for both phases of interest of ZnS and ZnSe. The Fermi energy is indicated by the horizontal line.

Note that at zero pressure (Figs. 2a and 2b), the top of the valence band is located at the point Γ and the lowest conduction band occurs at the same point. Hence, the material of interest is a (Γ- Γ) direct band gap semiconductor. The LDA band gap is found to be about 1.897 and 1.115 eV for ZnS and ZnSe, respectively. Our findings are underestimated with respect to the experimental ones of 3.82 eV [55] and 2.87 eV [56] reported for ZnS and ZnSe, respectively. This is an expected result since the LDA and GGA within DFT are known to yield underestimated band-gaps with respect to experiment [57–59]. At the pressure of transition (pt), the picture of the electronic structure seems to be similar to that at zero pressure for both ZnS and ZnSe materials. However, one can note a shift of all bands. The shift varies depending on the k point and energy. Even that, the semiconductor in question remains a (Γ- Γ) direct band-gap at P_t. Our calculation showed that the band gap increased with increasing pressure. It is found to be 2.411 and 1.624 eV for ZnS and ZnSe respectively at P_t. The valence bands seem to be less dispersive than the conduction ones. Similar trends have been reported by Bouarissa for $Ga_xIn_{1-x}As$ semiconductor ternary alloys [60] and InN semiconductor compound [61].

The electronic structures of rocksalt ZnS and ZnSe at Pt are illustrated in Figs. 3a and 3b. Note that the energy bands and the Fermi level are crossed and as a consequence the conduction and valence bands merge with each other. Hence, the rocksalt structure exhibits a metallic character for both ZnS and ZnSe. This agrees with the results of Smelyansky and Tse [23].

Structural parameters

In the zinc-blende case (Fm3m) of the materials under study, the Zn and S (Se) atoms locate at (0,0,0) and (1/4,1/4,1/4), whereas for the rocksalt (F4-3-m) structure, they are located at (0,0,0) and (1/2,1/2,1/2). An optimization technique is applied to obtain different structural parameters of ZnS and ZnSe. The computed total energies at several various volumes around equilibrium are fit using the Murnaghan equation of state [62] so as to determine the equilibrium lattice parameter and the bulk modulus for both zinc-blende and rocksalt ZnX (X = S,Se). Table 1 depicts the findings of our computations. It includes also the experimental and previously published theoretical results for comparison. Note that generally there is a reasonably good accord between the present results and those quoted in the literature. For zinc-blende structure, the lattice constants seem to be underestimated with respect to experiment whereas the bulk modulus appears to be overestimated. This is due to the used LDA approach.

The lattice parameter of the rocksalt phase is 4.988 Å for ZnS and 5.21 Å for ZnSe which agree with 5.06 Å [37] and 5.299 Å [21] for ZnS and ZnSe, respectively. The bulk moduli for zinc-blende and rocksalt ZnS (ZnSe) are 83.16 (68.54) and 102.93 (84.91) GPa, respectively. The accord between our findings regarding B_0 and experiment is reasonably well. The value of B_0 for the zinc-blende structure is much lower than

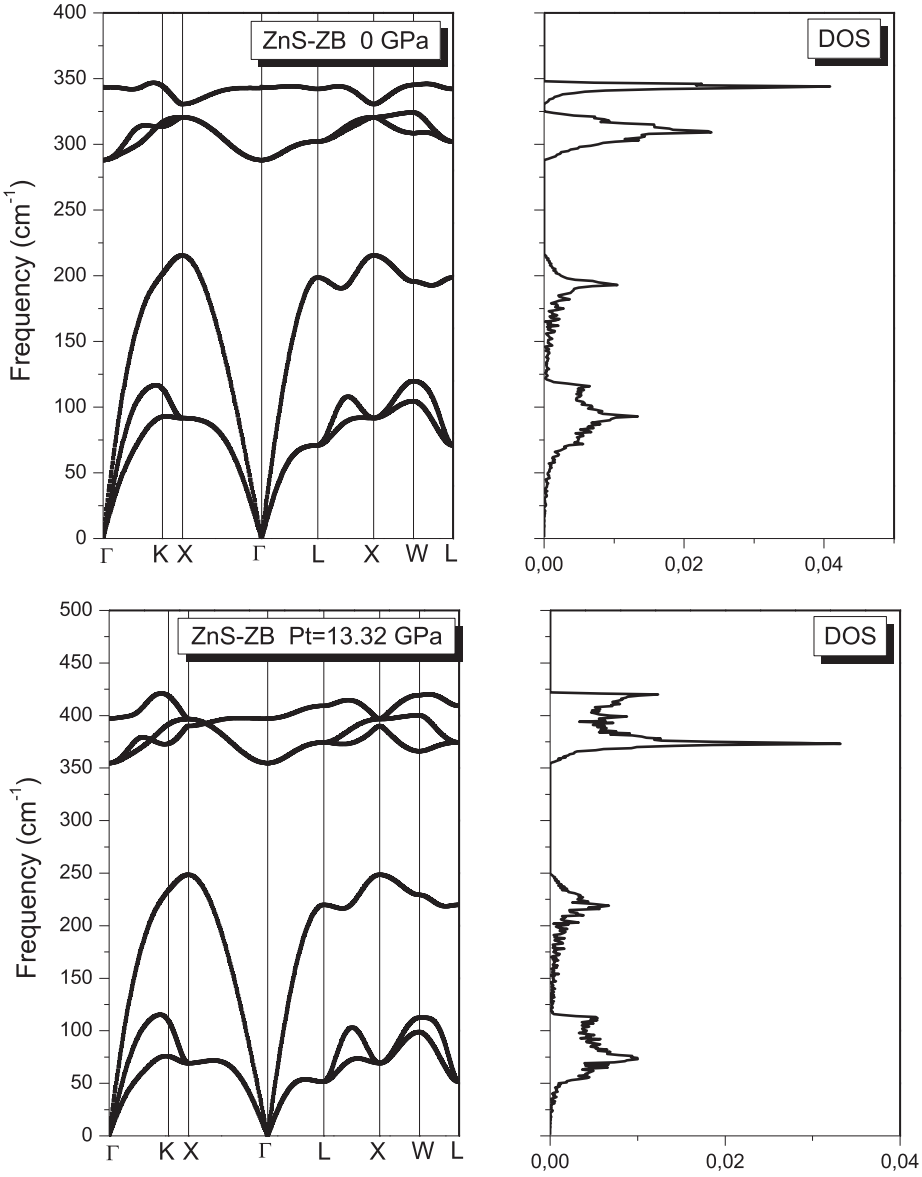

Fig. 4. Phonon-dispersion curves and the phonon density of states (DOS) for zinc-blende (ZB) ZnS at zero and 13.32 GPa pressure.

that of the rocksalt phase (B_0 increases by reducing the volume on going from zinc-blende → rocksalt). The same observation can be noticed for B'. By observing table 1 one can notice that the lattice parameter of zinc-blende ZnS is approximately 15% lower than that of ZnSe. On the other hand, the bulk modulus of ZnS seems to be higher than that of ZnSe reflecting the important hardness of ZnS with respect to that of ZnSe.

The pressure of transition (Pt) from zinc-blende to NaCl phase of the materials in question has been calculated from the common tangent of the two energy-volume curves of the two phases of interest. Pt is deduced from the slope of the tangent. It is known as the pressure of equal enthalpies of the two structures of interest. Our findings concerning Pt are 13.32 and 11.24 GPa for ZnS and ZnSe, respectively. These values appear to be slightly smaller than the experimental ones of 14.7 GPa [36] and 11.8 GPa [65] GPa quoted for ZnS and ZnSe, respectively.

Elastic properties

The elastic properties of semiconductors are useful quantities which provide important information about the nature of the forces operating in solids [66–69]. Upon compression, the elastic constants of the semiconducting materials are very important in predicting and understanding the material response, strength, mechanical stability and phase transitions. Nevertheless, so far only limited investigations have been conducted on the elastic properties of ZnS and ZnSe at high pressures, to the best of our knowledge. In fact, the cubic crystal is known to have three independent elastic constants C_{11}, C_{12} and C_{44}. In Table 2, we summarize our obtained C_{ij}'s for ZnS and ZnSe in both structures being considered in this work. For comparison, the experimental and previous theoretical data are also presented. Note that the deviation of our findings from those of experiment [71] is 4.64 (1.25),

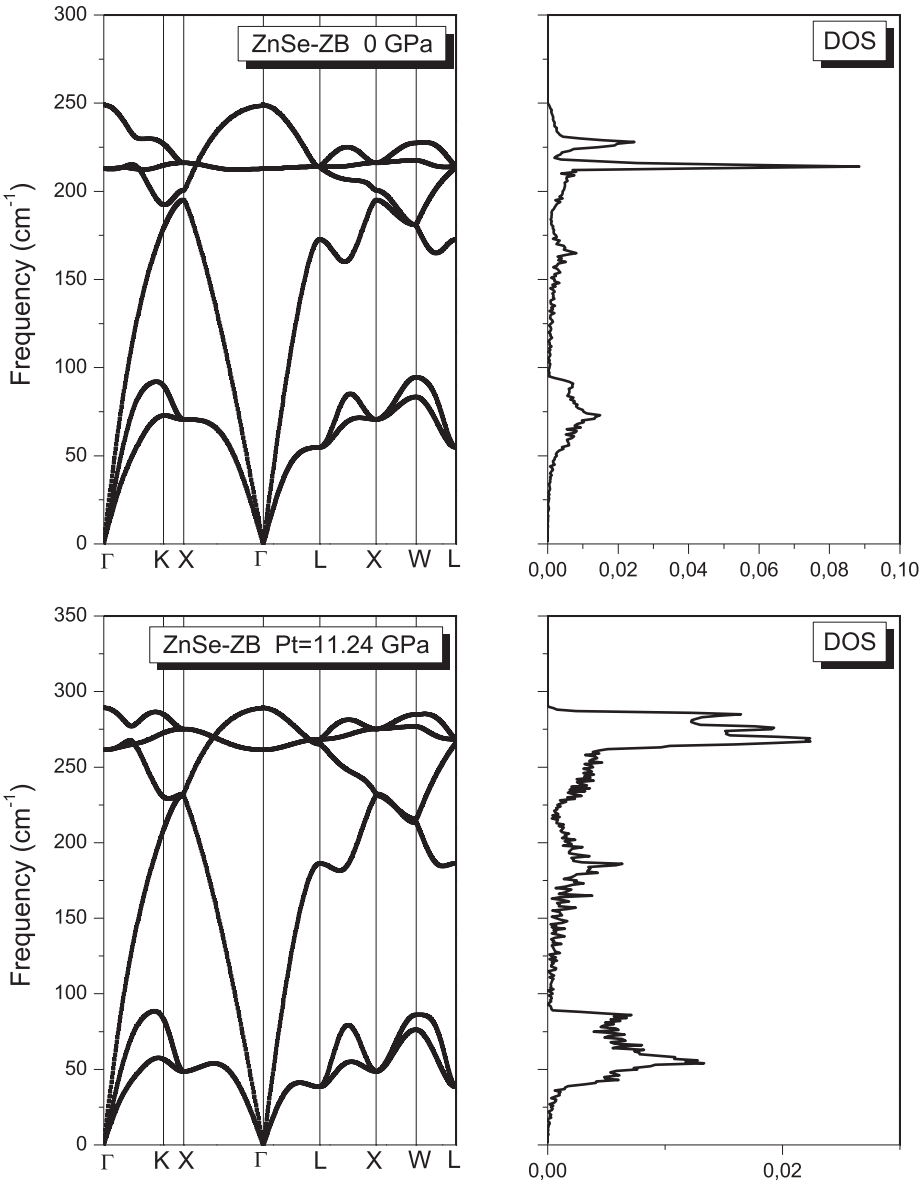

Fig. 5. Phonon-dispersion curves and the phonon density of states (DOS) for zinc-blende (ZB) ZnSe at zero and 11.24 GPa pressure.

4.89 (5.47) and 1.51 (12.61)% for C_{11}, C_{12} and C_{44} calculated for zinc-blende ZnS (ZnSe), respectively. These deviations from the experimental data are within the acceptable error bars that result from the use of the LDA approach. When comparing with previous calculated data, our values appear to be generally smaller than those obtained by Wang and co-workers [71]. The lattice parameter of zinc-blende ZnS is smaller than that of zinc-blende ZnSe. All C_{ij}'s of ZnS are higher than those of ZnSe. Because the C_{ij}'s of a material describe the stress needed to maintain a given deformation, we can say that zinc-blende ZnS is mechanically stronger than zinc-blende ZnSe. We observe that upon compression, C_{11} and C_{12} are enhanced whereas C_{44} is de-enhanced. This is true for both materials under consideration. For all obtained C_{ij}'s at any given pressure being considered here, the following sequence $C_{11} > C_{12} > C_{44}$ is observed for the compounds ZnS and ZnSe.

Phonon frequency

Phonons play an important role in understanding fundamental properties of solid materials [72–74]. The phonon spectra of semiconducting compounds ZnS and ZnSe have been computed using response-function approach and Fourier interpolation scheme as well as the density-functional perturbation theory (DFPT) [75]. The latter allows exact solutions of lattice dynamical frequencies in each point in the Brillouin zone. As a matter of fact, the implementation of perturbation theory into a density-functional framework has allowed the computation of the first-principles phonon dispersions in semiconducting materials [76,77] and metals [78,79].

Rocksalt and zinc-blende structures of semiconductors have two atoms per primitive unit cell, and therefore they have six phonon

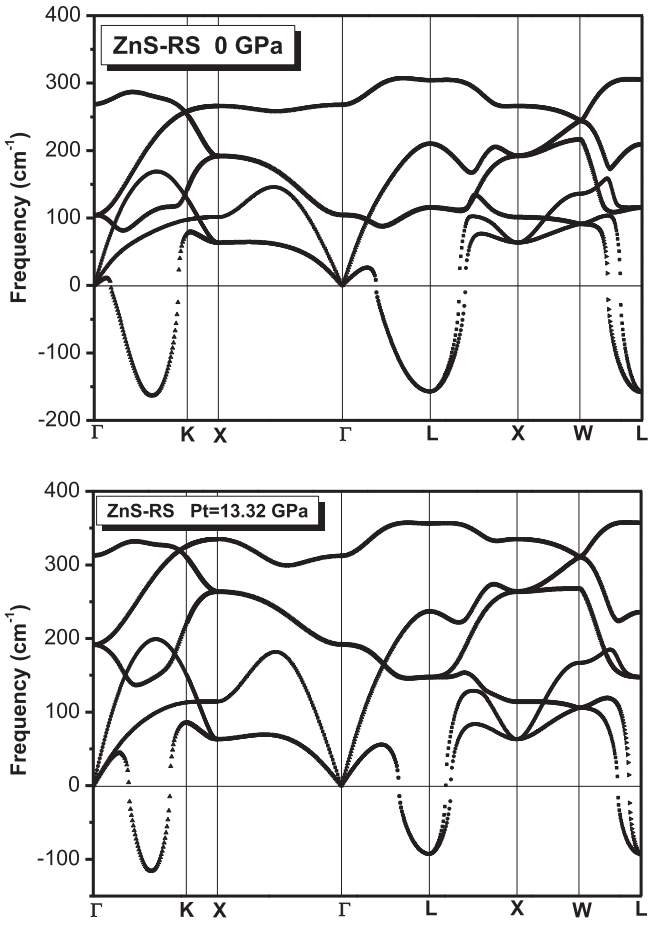

Fig. 6. Phonon-dispersion curves and the phonon density of states (DOS) for rocksalt (RS) ZnS at zero and 13.32 GPa pressure.

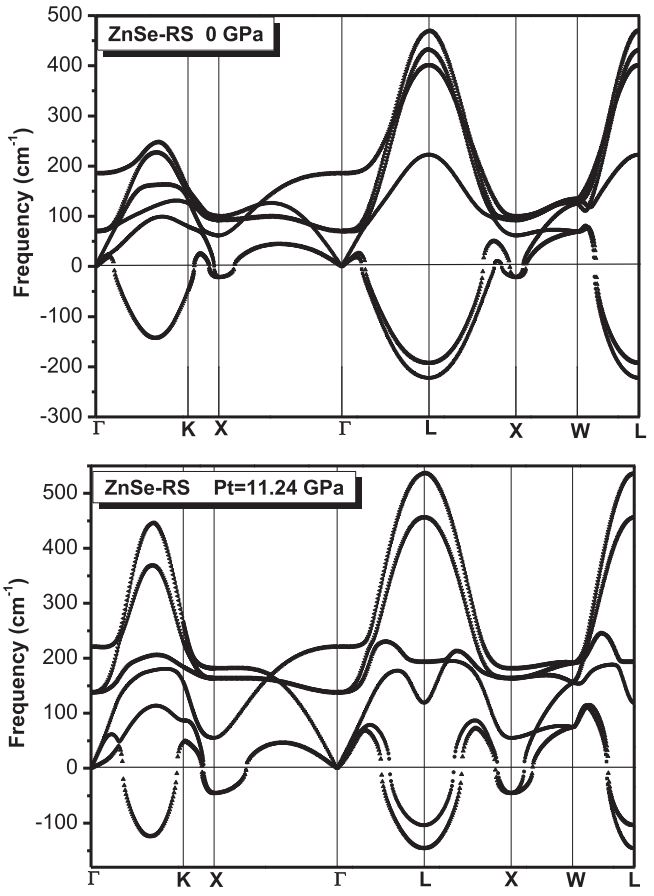

Fig. 7. Phonon-dispersion curves and the phonon density of states (DOS) for rocksalt (RS) ZnSe at zero and 11.24 GPa pressure.

branches. These branches are divided into three acoustic phonon branches and three optical phonon curves. Phonon spectra are computed along various high-symmetry directions in the Brillouin zone for given values of applied pressure. Our results are plotted in Figs. 4–7 for ZnS and ZnSe. Besides, the calculated phonon frequencies at high symmetry points in the Brillouin zone for zinc-blende and rocksalt phases of the materials of interest are depicted in Table 3 along with the existing data in the literature for comparison. In the case of zinc-blende ZnS, an overlap seems to appear between LA and TA branches. This corresponds to a vanishing gap that appears in the density of states (DOS) (Fig. 4). This feature seems to be not consistent with those reported for other III–V compound semiconductors [53]. The acoustic and optical branches for ZnS exhibit a gap between them. Nevertheless, no important overlap between LO and TO-phonon branches can be observed. The TO phonon frequency in zinc-blende crystals is lower than that of the LO phonons. This can be attributed to the partially ionic character of the bonding in zinc-blende crystals. In the case of Si, for example, where the bonding is purely covalent, the zone-center optical phonons are degenerate. The determined LO and TO frequencies at the Γ high-symmetry point are in accord with the Raman measurement. Their values are of 287.89 (212.66) and 343.49 (249.17) for LO and TO modes, for ZnS (ZnSe), respectively. These values agree as well with the theoretical ones reported previously in Refs. [24,81,82].

Although the phonon dispersion spectra seem to be qualitatively similar, one can note several distinctions in these spectra. These distinctions are believed to be due to the difference in the elastic forces strengths and the degree of the ionicity. For zinc-blende ZnSe, we note the absence of the gap between the acoustical and optical phonon branches (see Fig. 5). The TO and longitudinal-acoustical (LA) phonon branches are considerably overlapped.

This is due to the fact that the masses of Zn and Se atoms are almost the same. A noticeable flatness in one of the two TO phonon dispersion spectra can be observed. This corresponds to a sharp peak in the DOS (see Fig. 5).

In fact, the TA branches flatness over a wide range in the Brillouin zone is common for other II–VI semiconductors. This leads to the lack of the pronounced peaks in the one-phonon DOS. From the plotted partial DOS, the S (Se) atom (light atom) contributes essentially to the high frequency vibrations, whereas the Zn atom is expected to dominate the low frequencies. The pressure dependence of the frequencies at high symmetry points in the Brillouin zone is given in Table. 3. The phonon frequencies seem generally to be enhanced when pressure is applied for both phases of interest. The phonon-dispersion spectra of ZnS and ZnSe in the rocksalt structure are shown in Figs. 6 and 7, respectively. Also shown are the corresponding one-phonon DOS. Note that at zero pressure the phase of interest is dynamically unstable.

Table 3
Phonon frequencies for the high symmetry points in the Brillouin zone for ZnS and ZnSe in the zinc-blende and rocksalt phases.

Material	P(GPa)	Zinc-blende		Rocksalt		
		TO	LO	*TO*	LO	
ZnS	0	287.894	343.496	104.526	268.662	This work
		276 [80]	–			Expt.
		289 [24]	348 [81]			Theor.
	pt	354.581	397.3135	191.974	313.044	This work
ZnSe	0	212.663	249.173	71.076	185.735	This work
		213 [75]	253 [75]			Expt.
		216 [82]	252 [82]			Theor.
	pt	261.358	289.424	138.518	221.433	This work

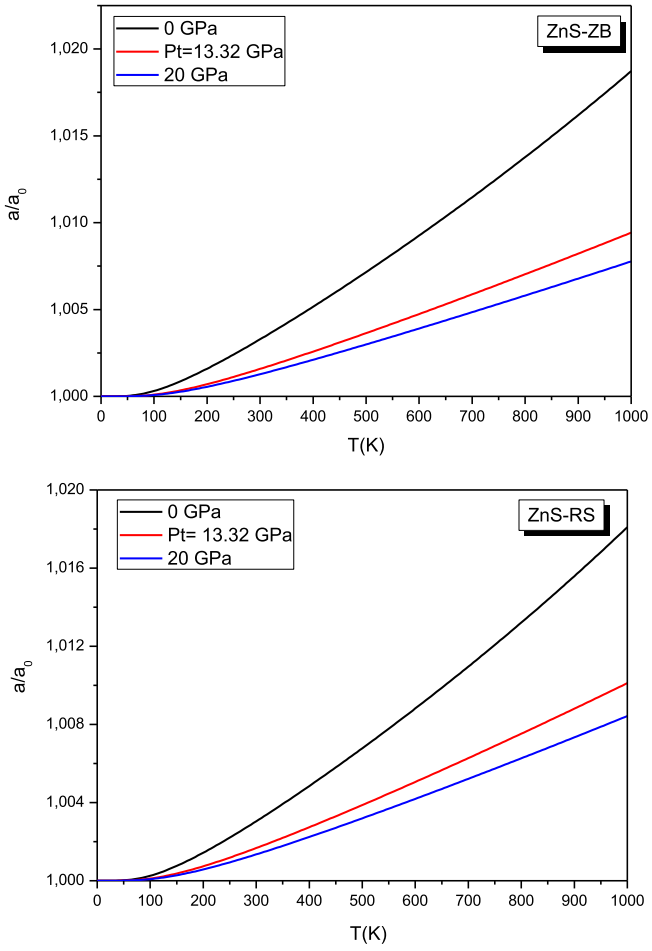

Fig. 8. Normalized lattice constant versus temperature for zinc-blende (ZB) and rocksalt (RS) ZnS for different given pressures.

Thermodynamic properties

The thermodynamic properties are among important basic properties of any semiconductor material. They are linked to the lattice dynamical behavior of solid materials. The accurate knowledge of these properties can provide information about the materials applications at various temperatures [83,84]. In this paper the thermodynamic properties of ZnS and ZnSe semiconductors at various pressures and temperatures have been studied using the quasi-harmonic Debye model. The considered temperature range is from 0 up to 1000 K at given pressures of 0, Pt and 20 GPa. The computation of the vibrational properties is an important tool for understanding the thermodynamic and several other solid material properties. Fig. 8 illustrates the variation in the lattice constant ratio and the bulk modulus ratio versus temperature for ZnS and ZnSe respectively in both zinc-blende and rocksalt structures. We observe that by raising the temperature, the lattice parameter ratios of interest are increased but decrease with increasing pressure. This can be traced back to the dilatation of lattice constants when the temperature is increased. The behavior appears to be nonlinear at low temperatures up to room temperature, then it seems to become almost linear up to a temperature of 1000 K.

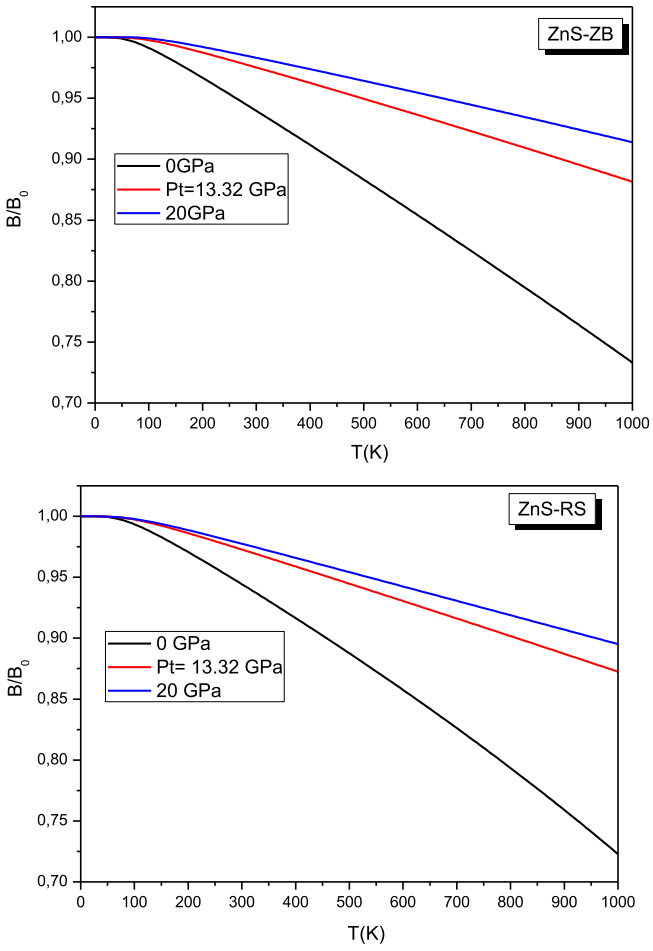

Fig. 9. Normalized bulk modulus versus temperature for zinc-blende (ZB) and rocksalt (RS) ZnS for different given pressures.

The origins for the differences in physical properties of the two semiconductors in question can be explored from the details of their inter-atomic combinations. This is not the case for the bulk modulus ratio as shown in Fig. 9. As a matter of fact, the bulk modulus is approximately invariant at any given pressure and for temperatures ranging from 0 to 120 K. Then it begins to decrease linearly for temperatures beyond 120 K. The de-enhancement of the bulk modulus ratio is believed to be due to

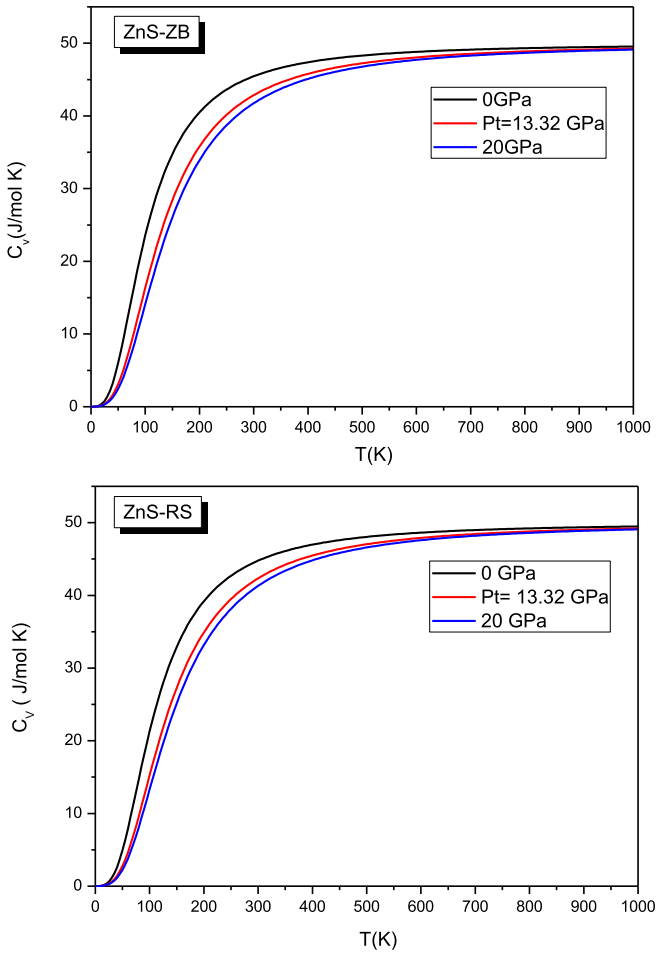

Fig. 10. Variation of the constant volume heat capacity versus temperature for zinc-blende (ZB) and rocksalt (RS) ZnS for different given pressures.

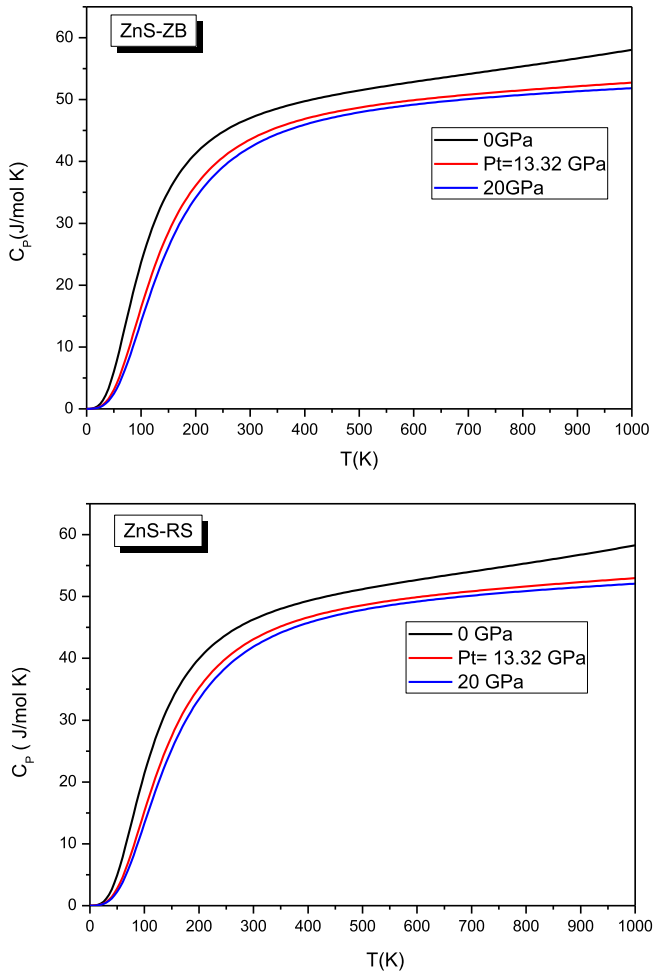

Fig. 11. Variation of the constant pressure heat capacity versus temperature for zinc-blende (ZB) and rocksalt (RS) ZnS for different given pressures.

the augmentation of the ionicity character by increasing the temperature leading to the reduction of the amount of bonding charge. Nevertheless, at a fixed temperature, it increases upon compression. Hence, the heat capacity at constant volume, C_V, is determined for various temperatures at a fixed pressure. The results obtained for ZnS and ZnSe are depicted in Fig. 10. We observe that for lower temperatures, C_v augments with raising temperature and decreases upon compression (C_V is proportional to T^3 [83]). However, at intermediate temperatures, the behavior of C_v is governed by the details of vibrations of the atom. At further elevated temperatures and for both phases being considered here, C_v approaches the limiting value 3R, whatever is the pressure in the range of interest, which agrees with the Dulong–Petit law [85]), where R is the perfect gas constant. Interestingly, ZnS is found to have lower C_V than ZnSe for all temperatures being considered here. This is attributed to its DOS for low-frequency modes.

Because of the thermal expansion caused by anharmonicity effects, C_P differs from C_V (Fig. 11). The C_P and C_V relationship is given by [86].

$$C_P - C_V = \alpha_V^2(T)B_0 \quad (1)$$

α_V in Eq. (1) is the volume thermal expansion coefficient, B_0 stands for the bulk modulus, V represents the volume and T is the absolute temperature. Entropy and enthalpy represent two useful concepts in thermodynamics. The entropy S accounts for the effects of irreversibility in thermodynamic systems. The variation of entropy is generally defined as a change in a more disorder state at a molecular level. The temperature dependence of S for both zinc-blende and rocksalt ZnS (ZnSe) is plotted in Fig. 12. We observe that at very small temperatures, S increases quickly with enhancing the temperature T for both structures being considered here. As a matter of fact, at sufficiently low temperatures, the vibrational excitations arise solely from acoustic vibrations. After a rapid increase, the functional dependence of S on T becomes more like a sub-linear behavior, i.e., S proportional to T^{α} with $\alpha < 1$. The same qualitative behavior was reported by Saib and coworkers [87] for InN in the rocksalt structure. On the other hand, the computed entropy increases by increasing the temperature and decreases upon compression. Interestingly, ZnS is found to have lower entropy than ZnSe for all temperatures being considered in this work. This is attributed to its DOS at low-frequency modes.

Conclusions

Using the DFT within the LDA along with response-function

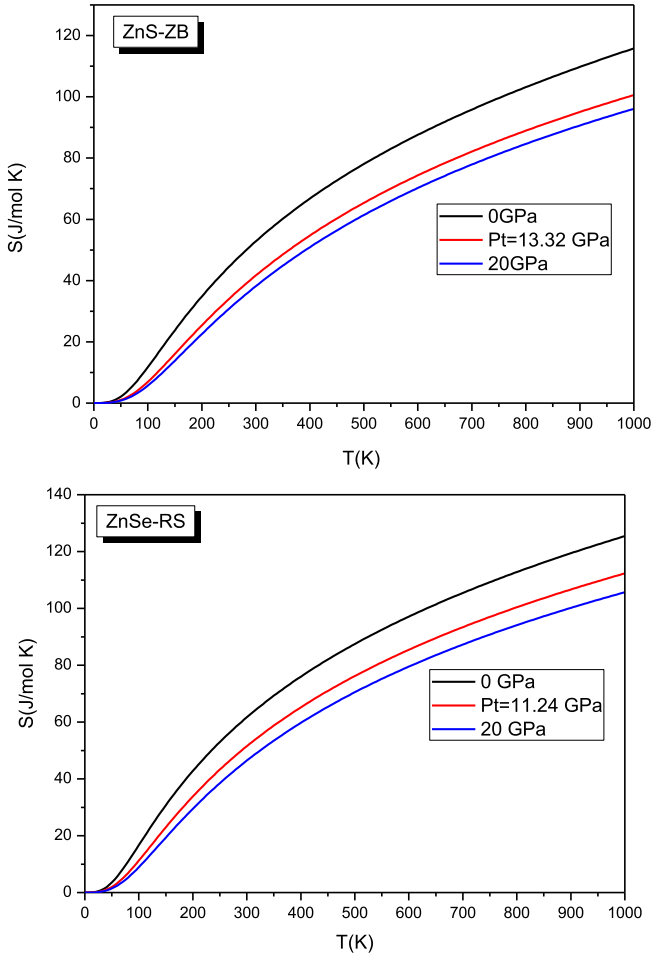

Fig. 12. Variation of the entropy versus temperature for zinc-blende (ZB) ZnS and rocksalt (RS) ZnSe for different given pressures.

calculations, the electronic structure and its derived properties such as structural, elastic, vibrational and thermodynamic properties of mono-chalcogenides ZnS and ZnSe semiconductor compounds in zinc-blende and rocksalt phases were investigated. Generally, our results showed a good accord with experiment and previous published theoretical values. The dependence on pressure of all properties being studied here was analyzed and discussed. Additionally, the effect of temperature on structural, entropy and heat capacity was examined and compared where possible with previous studies.

References

[1] Coe S, Woo WK, Bawendi M, Bulović V. Nature 2002;420:800.
[2] Tessler N, Medvedev V, Kazes M, Kan S, Banin U. Science 2002;295:1506.
[3] Gal D, Hodes G. Appl. Phys. Lett. 1998;73:3135.
[4] Huynh WU, Dittmer JJ, Alivisatos AP. Science 2002;295:2425.
[5] Colvin VL, Schlamp MC, Alivisatos AP. Nature 1994;370:354.
[6] Dabbousi BO, Bawendi MG. Appl. Phys. Lett. 1995;66:1316.
[7] O'Regan B, Grätzel M. Nature 1991;353:737.
[8] Greenham NC, Peng X, Alivisatos AP. Synth. Met. 1997;84:545.
[9] Wang K, Si N, Zhang Y-L, Zhang F, Guo A-B, Jiang W. Vacuum 2019;165:105.
[10] Wang K, Jiang W, Chen J-N, Huang J-Q. Superlattices Microstruct. 2016;97:116.
[11] Al-Douri Y, Hashim U. J. Ren. Subst. Energy 2014;6:013109.
[12] Al-Douri Y, Khachai H, Khenata R. Mater. Sci. Semicond. Process. 2015;39:276.
[13] C.G. Van de Walle (Ed.), Wide-band-gap Semiconductors, North Holland, Amsterdam, 1993 (also published as Physica B 185 (1993) 1).
[14] Jaiswal JK, Mattoussi H, Mauro JM, Simon SM. Nat. Biotechnol. 2003;21:47.
[15] Hannachi L, Bouarissa N. Phys. B 2009;404:3650.
[16] Rabah M, Abbar B, Al-Douri Y, Bouhafs B, Sahraoui B. Mater. Sci. Eng., B 2003;100:163.
[17] Al-Douri Y, Verma KD, Prakash D. Superlattices Microstruct. 2015;88:662.
[18] Benmakhlouf F, Bechiri A, Bouarissa N. Solid State Electron. 2003;47:1335.
[19] Grebe G, Roussos G, Schulz H-J. J. Phys. C: Solid State Phys. 1976;9:4511.
[20] Neumark GF, Park RM, DePuydt JM. Phys. Today 1994;47:26. and references therein.
[21] Karzel H, Potzel W, Köfferlein M, Schiessl W, Steiner M, Hiller U, Kalvius GM. Phys. Rev B 1996;53:11425.
[22] Qteish A, Muñoz A. J. Phys.: Condens. Matter 2000;12:1705.
[23] Smelyansky VI, Tse JS. Phys. Rev B 1995;52:4658.
[24] Agrawal BK, Yadav PS, Agrawal S. Phys. Rev. B 1994;50:14881.
[25] Chen R, Li XF, Cai LC, Zhu J. Solid State Commun. 2006;139:246.
[26] Nourbakhsh Z. J. Alloy. Compd. 2010;505:698.
[27] Ferahtia S, Saib S, Bouarissa N, Benyettou S. Superlatt. Microstruct. 2014;67:88.
[28] Casali RA, Christensen NE. Solid State Commun. 1998;108:793.
[29] Ackland GJ. Rep. Prog. Phys. 2001;64:483. and references therein.
[30] Bouarissa N. Mater. Chem. Phys. 2002;73:51.
[31] Saib S, Bouarissa N. Phys. Stat. Sol. (b) 2007;244:1063.
[32] Saib S, Bouarissa N, Rodríguez-Hernández P, Muñoz A. Phys. B 2008;403:4059.
[33] Daoud S, Bioud N, Bouarissa N. Mater. Sci. Semicond. Process. 2015;31:124.
[34] Smith PL, Martin JE. Phys. Lett. 1965;19(1965):541.
[35] Nelmes RJ, McMahon MI. Structural transitions in the group IV,III-V, and II-VI semiconductors under pressure chapter 3 volume 54 of Semiconductors and Semimetals,Academic Press; 1998. p. 145–246.
[36] Uchino M, Mashimo T, Kodama M, Kobayashi T, Takasawa E, Sekine T, et al. J. Phys. Chem. Solids 1999;60:827.
[37] Ves S, Schwarz U, Christensen NE, Syassen K, Cardona M. Phys. Rev. B 1990;42:9113.
[38] Zhou Y, Campbell AJ, Heinz DL. J. Phys. Chem. Solids 1991;52:821.
[39] Jaffe JE, Pandey R, Seel MJ. Phys. Rev. B 1993;47:6299.
[40] Balchan AS, Drickamer HG. Rev. Sci. Instrum. 1961;32:308.
[41] Drickamer HG. Rev. Sci. Instrum. 1970;41:1667.
[42] Tiong SR, Hiramatsu M, Matsushima Y, Ito E. Jpn. J. Appl. Phys. 1989;28:291.
[43] Adachi S. Properties of Group-IV, III-V, and II-VI Semiconductors. Chichester: Wiley; 2005.
[44] Zhao J. Phy. Lett. A 2007;360:645.
[45] Gangadharan R, Jayalakshmi V, Kalaiselvi J, Mohan S, Murugan R, Palanivel B. J. Alloy. Compd. 2003;359:22.
[46] Gonze X, Beuken J-M, Caracas R, Detraux F, Fuchs M, Rignanese G-M, et al. Comput. Mater. Sci. 2002;25:478.
[47] Ceperley DM, Alder MJ. Phys. Rev. Lett. 1980;45:566.
[48] Troullier N, Martins JL. Phys. Rev. B 1997;43:1993.
[49] Monkhorst HJ, Pack JD. Phys. Rev. B 1976;13:5188.
[50] Baroni S, Giannozi P, Testa A. Phys. Rev. Lett. 1987;58:1861.
[51] Bouarissa N, Saib S. J. Appl. Phys. 2010;108:113710.
[52] Karch K, Bechstedt F, Pavone P, Strauch D. Phys. Rev. B 1996;53:13400.
[53] Saib S, Bouarissa N, Rodríguez-Hernández P, Muñoz A. J. Appl. Phys. 2008;103:013506.
[54] Ferahtia S, Saib S, Bouarissa N. Intern. J. Mod. Phy. B 2016;30:1650147.
[55] Strehlow WH, Cook EL. J. Phys. Chem. Ref. Data 1973;2:163.
[56] Gürel HH, Akinci Ö, Ünlü H. Superlattices Microstruct. 2012;51:725.
[57] Lee S-G, Chang KJ. Phys. Rev. B 1995;52:3.
[58] Lin CM, Chuu DS, Yang TJ, Chou WC, Xu JA, Huang E. Phys. Rev B 1997;55:13641.
[59] Saib S, Bouarissa N. J. Phys. Chem. Sol. 2006;67:1888.
[60] Bouarissa N. Phys. Lett. A 1998;245:285.
[61] Bouarissa N. Eur. Phys. J. B 2002;26:153.
[62] Murnaghan FD. PNAS 1944;30:244.
[63] Madelung O. Numerical Data and Functional Relationships in Science and Technology, New Series, 17b. Berlin: Springer-Verlag; 1982.
[64] Yu PY, Cardona M. Fundamentals of Semiconductors Physics and Materials Properties. Berlin: Springer-Verlag; 2001 (Chapter 7).
[65] Nelmes RJ, McMahon MI, Wright NG, Allan DR. J. Phys. Chem. Solids 1995;56:545.
[66] N. Bouarissa, K. Kassali, Phys. Stat. Sol. (b) 228 (2001) 663; Phys. Stat. Sol. (b) 231 (2002) 294.
[67] Kim K, Lambrecht WRL, Segall B. Phys. Rev. B 1996;53:16310.
[68] Bouarissa N, Annane F. Mater. Sci. Eng., B 2002;95:100.
[69] Bouarissa N. Mater. Chem. Phys. 2006;100:41.
[70] Lee BH. J. Appl. Phys. 1970;41:2988.
[71] Wang HY, Cao J, Huang XY, Huang JM. Condens. Matter Phys. 2012;15:1.
[72] Baroni S, de Gironcoli S, Dal Corso A, Giannozzi P. Rev. Mod. Phys. 2001;73:515.
[73] Bouarissa N, Bougouffa S, Kamli A. Semicond. Sci. Technol. 2005;20:265.
[74] Bouarissa N. Phys. B 2011;406:2583.
[75] Hennion B, Moussa F, Pepy G, Kunc K. Phys. Lett. A 1971;36:376.
[76] Karch K, Bechstedt F. Phys. Rev. B 1997;56:7404.
[77] Saib S, Bouarissa N, Rodríguez-Hernández P, Muñoz A. Semicond. Sci. Technol. 2007;24:025007.
[78] Debernardi A, Alouani M, Dreyssé H. Phys. Rev. B 2001;63:064305.
[79] de Gironcoli S. Phys. Rev. B 1995;51:6773.
[80] Vagelatos N, Wehe D, King JS. J. Chem. Phys. 1974;60:3613.
[81] Chang IF, Mitra SS. Phys. Rev. 1968;172:924.
[82] Hamdi I, Aouissi M. Phys. Rev B 2006;73:174114.
[83] Debye P. Ann. Phys. 1912;39:789.
[84] Daoud S, Bouarissa N. Comput. Condens. Matter 2019;19:e00359.
[85] Mehl MJ. Phys. Rev. B 1993;47:2493.
[86] Callen HB. Thermodynamics and an Introduction to Thermostatistics. New York: Wiley; 1985.
[87] Saib S, Bouarissa N, Rodríguez-Hernández P, Muñoz A. Comput. Mater. Sci. 2014;81:374.